

Ruthenium behaviour under air ingress conditions: main achievements in the SARNET project

P. Giordano², A. Auvinen¹, G. Brillant², J. Colombani², N. Davidovich³, R. Dickson⁴, T. Haste⁶, T. Kärkelä¹, J.S. Lamy⁷, C. Mun², D. Ohai⁸, Y. Pontillon⁵, M. Steinbrück⁹, and N. Vér¹⁰

CONTRACT SARNET FI60-CT-2004-509065

- | | |
|----------------------------|---|
| 1) VTT Energy, Espoo (Fin) | 6) Paul Scherrer Institute, Villigen (CH) |
| 2) IRSN, Cadarache (Fr) | 7) EDF R&D, Clamart (Fr) |
| 3) ENEA, Roma (I) | 8) INR, Pitesti (Rom) |
| 4) AECL, Chalk River (Can) | 9) FzK, Karlsruhe (G) |
| 5) CEA, Cadarache (Fr) | 10) KFKI AEKI, Budapest (Hun) |

Summary

In a hypothetical severe accident in a Pressurized Water Reactor (PWR), Fission Products (FPs) can be released from the overheated nuclear fuel and partially transported by gases, composed of a mixture of superheated steam and hydrogen, to the reactor containment. Subsequent air ingress into a damaged reactor core may lead to enhanced fuel oxidation, affecting some FP release, especially to increase that of ruthenium. Ruthenium is of particular interest because of its high radio-toxicity and due to its ability to form very volatile oxides. In the reactor containment, such volatile forms are very hazardous as they are much less efficiently trapped than particulate forms by emergency filtered venting.

In the four and a half years of SARNET, collaborative research dedicated to the “ruthenium story” has been performed by several partners. This paper presents the main achievements over the whole project period.

Starting from experimental observations showing that fuel could be oxidized by air to a high extent, and that a significant fraction of ruthenium inventory can be released, rather satisfactory models have been developed. Besides, the effect of the air interaction with Zircaloy cladding, as well as with UO₂ itself, has been studied.

Experiments on complex transformations of ruthenium oxides upon cooling through the reactor circuit have been performed. An unexpected significant effect of temperature on the decomposition rate of gaseous ruthenium compounds has been found, as well as effects of the nature of circuit internal surfaces and other FP deposits. So it has been highlighted that various forms of ruthenium can reach the containment, but the most probable gaseous species under these conditions is ruthenium tetroxide. Preliminary analysis of ruthenium transport supports these conclusions.

Experiments and analysis have also been launched on the radio-chemical reactions undergone by these ruthenium oxides in the reactor containment. Competing effects of gaseous decomposition to solid particles and re-volatilization from these ruthenium deposits have been demonstrated and modelled.

The paper concludes by identifying the remaining work needed to achieve full resolution of the ruthenium source term issue. Recommendations are made for future research activities in a possible follow-up programme.

Source Term and Containment Issues, Paper 3.9**A. INTRODUCTION**

Since more than a decade ago, experiments have shown (Ref. [1]) that when air is in contact with irradiated UO_2 fuel, the latter and its Fission Products (FPs) can undergo oxidation, especially under high temperature conditions. Some FPs, which were known to be weakly released during severe accident progression in a reactor core under *steam* oxidizing conditions, may form highly volatile oxide species under *air* oxidizing conditions, and thus give enhanced release. At the start of SARNET, 4 years ago, some gaps in understanding were still identified, such as knowledge of accident situations in which air can come into contact with hot UO_2 fuel, missing predictive models for FPs release kinetics under these conditions, potential for these FPs to be transported out of the reactor coolant system into the containment and their potential to remain in the gas phase there, in which form they would only be retained by filters to a very limited extent. It was then a challenge for the Source Term topical area of SARNET to address these questions.

Circumstances in which air can come in contact with irradiated fuel were studied in the first two SARNET years and (Refs. [2], [3]) provide a synthesis of this work, so will not be reported here. What was subsequently investigated in more detail was the *effect* of such air ingress on the core materials: remaining cladding material oxidation and degradation, UO_2 “decrepitation” for core areas of low temperature (below ~ 1800 K), where fuel may undergo phase change (UO_2 to U_3O_8 , see Ref. [4]). Section B1 presents new progress in this area.

Concerning FPs release kinetics, the key fission product of interest in these circumstances is ruthenium, since its radiotoxicity is particularly high and its behaviour varies greatly depending on the surrounding temperature and oxygen potential (Ref.[5]). Recent attempts to model its release kinetics (Ref. [3]) were not completely convincing and thanks to new experimental data and deeper analysis of already available ones, an improved approach is proposed in Section B2.

Ruthenium volatile oxide species may remain relatively stable even when passing through lower temperature areas in the primary circuit, as already reported in the first SARNET years (Refs. [2], [3]), and thus may reach the reactor containment under gaseous forms, and then may potentially be released to the outside environment. Recent efforts have been carried out to understand better the thermodynamic behaviour along this path, based on additional experiments and an overall interpretation of available results (Section B3).

The final concern of this “ruthenium story” is the trapping efficiency of the reactor containment building, and especially of the trapping on the containment surfaces and in the sump. This is linked with the question whether ruthenium volatile oxides keep chemically stable in the containment, while being submitted to significant radiation. Section B4 summarises the main achievements on this particular topic.

B. MAIN ACHIEVEMENTS**B.1 Effect of an air ingress on clad and fuel degradation**

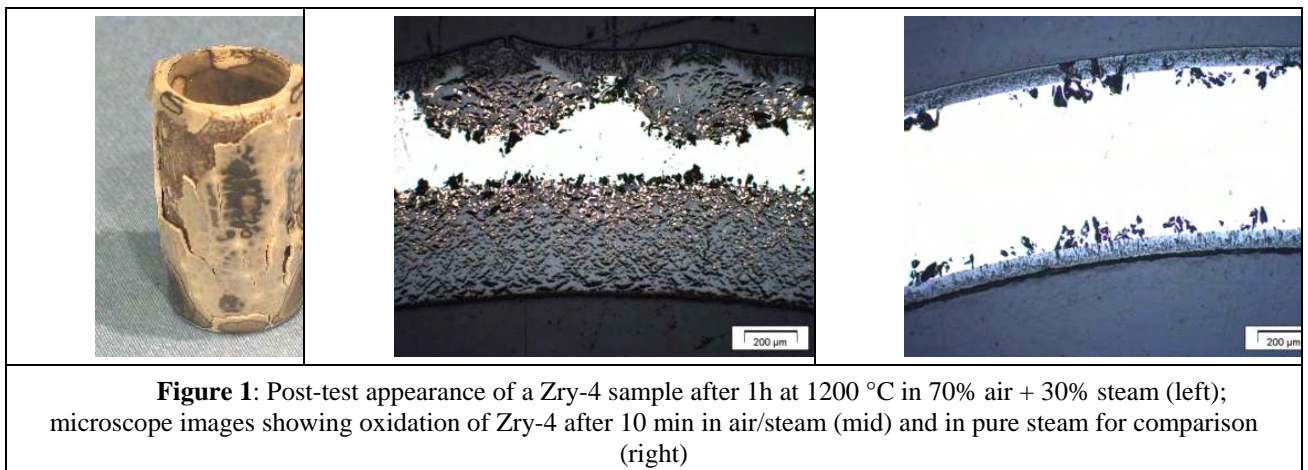
Extensive experimental work on the oxidation of Zircaloy cladding has been performed under prototypical conditions for air ingress during an hypothetical severe nuclear reactor accident, i.e. at temperatures in the range 800 - 1500°C and consideration of mixed air(nitrogen)-steam atmospheres and pre-oxidation (Ref. [6]). This work is mainly coordinated under the Corium topic of SARNET; a brief summary is given here.

Source Term and Containment Issues, Paper 3.9

The oxidation in air as well as in air and nitrogen-containing atmospheres leads to strong degradation of the cladding material. The main mechanism for this process is the formation of zirconium nitride and its re-oxidation. The different densities of Zr, ZrO_2 , and ZrN cause volume mismatches, compressive stress build-up and relief by crack formation leading to porous, non-protective oxide scales (Figure 1). From a safety point of view, the barrier effect of the fuel cladding is lost much quickly than during accident transients under only steam atmosphere. The high exothermal energy of the oxidation of zirconium alloys in air on the one hand and low cooling effect of air compared to steam on the other hand cause early temperature escalations from comparatively low temperatures as was seen during the preparation and conduct of the QUENCH-10 bundle test on air ingress (Ref. [7]).

However, it has been found that pre-oxidation in steam prevents air attack as long as the oxide scale is intact, i.e. at temperatures above 1050 °C (beyond breakaway regime) and as long as oxidising gases are available (no steam starvation conditions).

Regarding modelling of air ingress in severe accident computer codes one conclusion is that parabolic correlations for oxidation in air may be applied only for high temperatures (>1400 °C) and for pre-oxidized cladding (≥ 1100 °C). For all other conditions, faster, i.e. more linear reaction kinetics should be applied.



The associated modelling work, which is based on the FZK separate-effects tests and similar data from IRSN, which is being performed by IRSN, GRS, PSI and EdF, is also coordinated within the Corium area and is reported separately (Ref. [8]). There has been some success in reproducing the transition from parabolic to linear kinetics as the protective effect of the oxide scale degrades. An example is given, see figure 2, showing predictions of the prototype PSI model in comparison with FZK thermobalance data, showing the effect of pre-oxidation in oxygen before air ingress. Further work is in progress, and extension to advanced cladding materials is being considered.

Source Term and Containment Issues, Paper 3.9

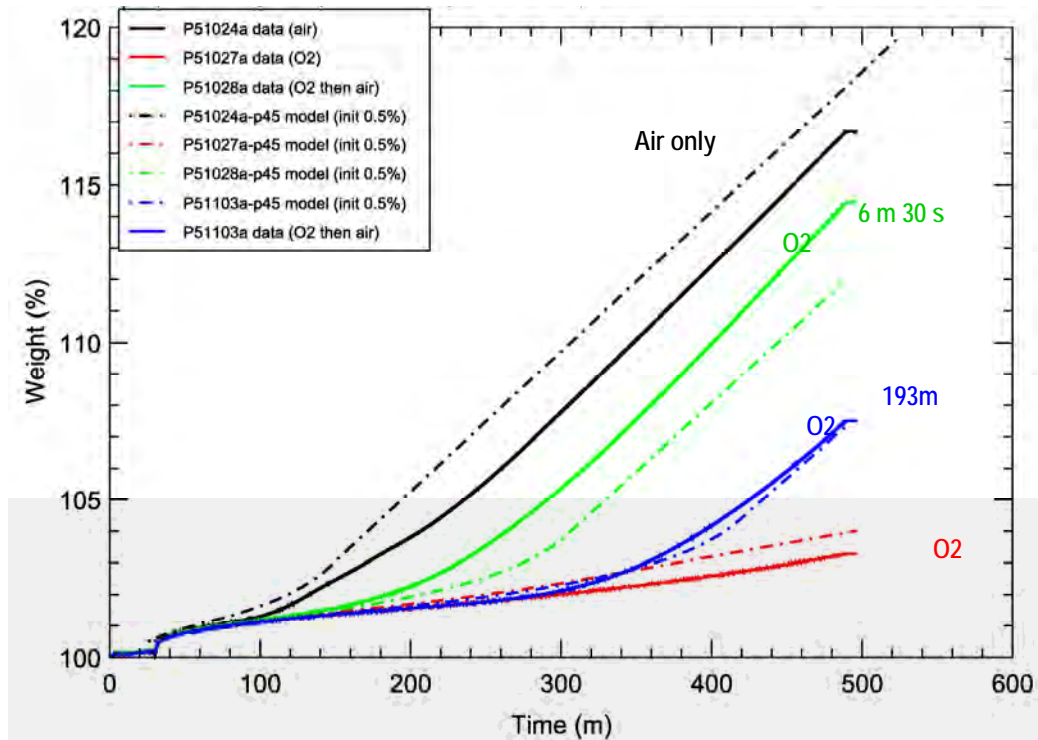
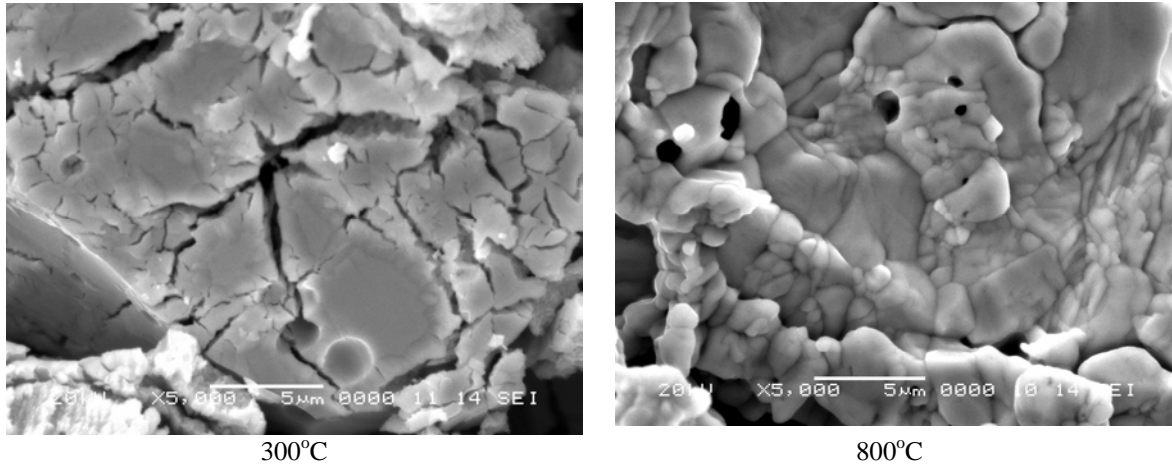


Figure 2: Comparison of predictions of the PSI Zircaloy/air oxidation model with FZK separate-effects weight gain data, showing the effect of pre-oxidation in oxygen

Beyond cladding oxidation and subsequent cladding degradation, fuel will be exposed to air oxidation as well. In SARNET, the oxidation and degradation of fuel have been experimentally investigated at INR (Ref. [9]). The first step of the experimental programme was performed in the temperature range 300-1400°C. A thermobalance and dedicated analysis equipment (Ref. [10]) were used to measure UO_2 pellets self-disintegration rates, grain (fragment) size distribution and micro-scale characteristics.

Based on these measurements, an interpretation of the mechanisms involved in UO_2 self-disintegration by air oxidation has been proposed (Ref. [11]). At first, the attack on the pellet surface detaches small fragments. When the first layer is removed, open pores and cracks appear on the surface allowing deeper oxygen diffusion inside the pellets. UO_2 transformation into U_3O_8 induces very strong stresses. The attack in cracks and pore zones produces dislocations of large fragments. Since the surface area increases with pore and crack formation, the disintegration rate increases too. The large fragments are broken into smaller fragments and so on (see figure 3 - 300°C). As temperature increases, a new phenomenon appears: the sintering of U_3O_8 formed by UO_2 oxidation. Necks and bridges formed between the fragments by sintering connect the pieces (see figure 3 - 800°C). During fuel oxidation, these two phenomena take place competitively. At low temperatures, self-disintegration of sintered pellets by oxidation is predominant and a very fine powder is observed (<32µm). At high temperature, the U_3O_8 sintering rate is high enough for large fragments to be formed (>200 µm). The experimental work will be continued with studies of oxidation of sintered pellets in steam-air atmospheres and of ruthenium release from sintered pellets.



300°C
800°C
Figure 3: Micro-scale observations of fuel fragments

B.2 Ruthenium release from fuel

Inside the fuel, FPs will also be affected by air oxidation, and among them, ruthenium. Many complex phenomena are involved in ruthenium release from fuel. As a matter of fact, one can observe that, depending on which experimental tests are considered, this fission product may be classified either amongst low or high volatile fission product groups. More precisely, in reducing or somewhat oxidizing conditions, ruthenium is released in quite small quantities. For example, the ruthenium fraction released from fuel is about 5% in most VERCORS tests (Ref. [12]). On the other hand, ruthenium is almost completely released at a very rapid rate under air ingress as observed in some CRL tests (Refs. [19] to [23]). One can remark that ruthenium can also be highly released in steam atmospheres such as in the VERCORS HT2 test (in which fuel oxygen potential reached high values, and the test temperature was high).

The proposed modelling of ruthenium release from fuel is based on a thermodynamic approach of ruthenium volatilization from either metallic or oxide ruthenium precipitates (Ref. [13]). It has been observed that this modelling leads to quite good results on experiments with UO_2 fragments [Ref. 3]. However, it has also been recognized that the estimation of ruthenium release from clad samples had to be improved.

As ruthenium release is highly sensitive to fuel oxygen potential, one should carefully evaluate this parameter during test calculations. Furthermore, it has been noticed that oxygen diffusion in fuel is a key stage of fuel oxidation under air ingress at high temperatures. Since this phenomenon was not taken into account in the ASTEC/ELSA code, it has been decided to take it into account in the new modelling. The analytical basis has been that of the fuel oxidation model implemented in the MFPR code (Ref. [14]). This modelling takes into account oxygen diffusion within the UO_2 matrix, effects of oxygen exchange at the gas/solid interface and of mass transfer in the multi-component gas phase (Ref. [15]).

Together with this modelling improvement, new correlations have been implemented for the evolution, with temperature and fuel stoichiometric deviation, of both fuel oxygen potential and oxygen diffusion coefficient in fuel. For the latter, the correlation of Ramirez et al. (2006) (Ref. [16]) has been retained since it takes into account the most recent experimental measurements (Ref. [17]) with a direct dependence of D (m^2s^{-1}) on temperature and fuel stoichiometric deviation:

$$\log(D(T, x)) = -9.386 - \frac{4.26 \cdot 10^3}{T} + 1.2 \cdot 10^3 T x + 7.5 \cdot 10^{-4} T \log\left(\frac{2+x}{x}\right)$$

Source Term and Containment Issues, Paper 3.9

Concerning fuel oxygen potential, Labroche et al. (Ref. [18]) performed useful measurements and proposed a correlation based on tabulated parameters. For easier implementation in simulation tools like ASTEC, a new correlation for fuel oxygen potential has been developed on the basis of these experimental measurements:

$$\Delta GO_2 = 8.31 T \left[17.38 (2 + x) - 22.55 + 2 \ln \left(\frac{x}{1-x} \right) - \frac{34500}{T} \right]$$

With this new modelling of fuel oxidation and new correlations, calculations of AECL tests have been carried out. At first, non-regression tests have been simulated to check that calculated results of experiments involving UO₂ fragments are still in good agreement with experimental measurements on MCE1 (Ref. [19]) (see figure 4). Then, simulations of release from clad samples showed improvements in comparison with the previous study (Ref. [3]). For example, the ruthenium release calculation for test HCE3-H02 (Ref. [20]) (see figure 5) has been enhanced in comparison with the previous study (Ref. [3]).

Recently, the validation database has been extended with additional AECL tests on two UO₂ fragments, UCE12-T02 and UCE12-T15 (Ref. [21]) and two clad samples, HCE1-M17 and HCE2-LM4 (Ref. [22]). Temperature and test environment profiles for these tests are shown in figures 6 and 7, respectively, together with Ru and Cs fractional release measurements. These tests were conducted by inserting the sample into a pre-heated furnace in flowing inert gas (purified Ar, or Ar/2% H₂), then subjecting the sample to air, or to steam followed by air. In UCE12 test T02, Cs release occurred rapidly when the sample was subjected to steam environment, but statistically significant Ru release did not occur until air was added. In UCE12 test T15, release of Ru at 1898 K was significantly slower than releases at lower temperatures in other tests (including UCE12 test T02). The rate decrease in the 1670 K to 1970 K temperature region has been attributed (Ref. [23]) to an increase in uranium oxide plasticity in this region, which could limit the mass transfer of Ru out of the sample. HCE1 test M17 was conducted on a clad segment of CANDU-type fuel with a Zircaloy end-cap on the downstream end only. Note that Cs release increased immediately after air contacted the sample because of the partial exposure of the UO₂ to the gas stream, but Ru release did not increase until about 3000 s later. HCE2 test LM4 was conducted on a clad segment of PWR fuel rod with press-fitted Zircaloy end-caps on both ends. Note that statistically significant Ru release did not occur during HCE2 test LM4, despite maintaining the sample at test temperature in air for more than 4000 s after the increase in Cs release rate, which indicated contact of air with the UO₂. This low release may be due to limitation of Ru and air mass transfer by the fully oxidized cladding.

One can observe a good agreement between experiments and calculations with the new modelling for these four tests with well estimated released kinetics and final release rate of ruthenium. In conclusion, it appears that ruthenium release modelling with use of the new model of fuel oxidation under air ingress developed in SARNET frame is satisfying. A next step will consist in applying this modelling to a higher burn-up UO₂ fuel exposed to air, through a comparison with the so-called "Ru scoping experiment" performed in SARNET by CEA in the MERARG facility [3]. In this experiment, the sample, one pellet including its cladding, was taken from UO₂ fuels irradiated during six cycles in PWR (i.e. up to 72 GWd/t_m) operated by EDF. The sample was heated up from room temperature up to 1350°C (temperature ramp of 0.2°C/s) under air flow, and the temperature was then maintained at 1350°C during 40 minutes.

Source Term and Containment Issues, Paper 3.9

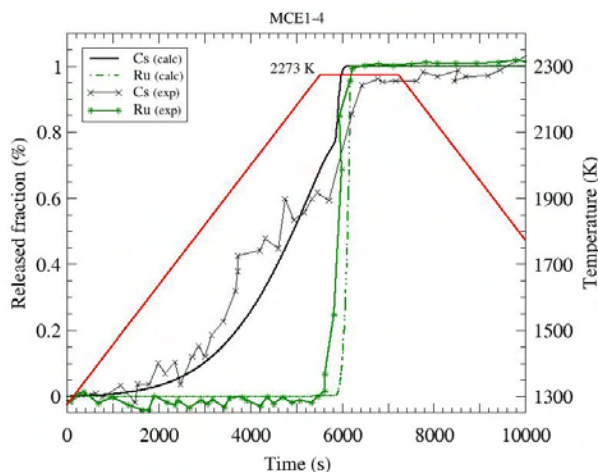


Figure 4: Release kinetics of Cs and Ru for test MCE1-4

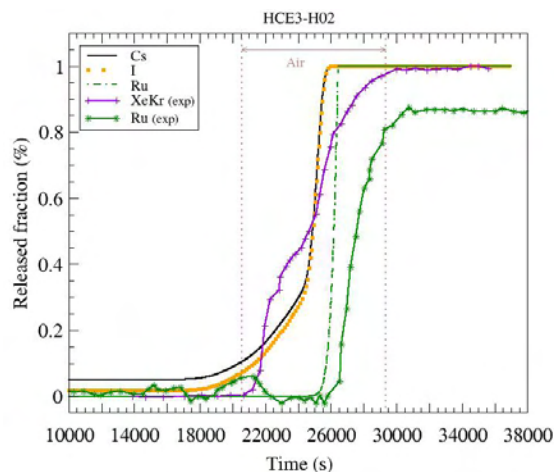


Figure 5: Release kinetics of Cs and Ru for test HCE3-H02.

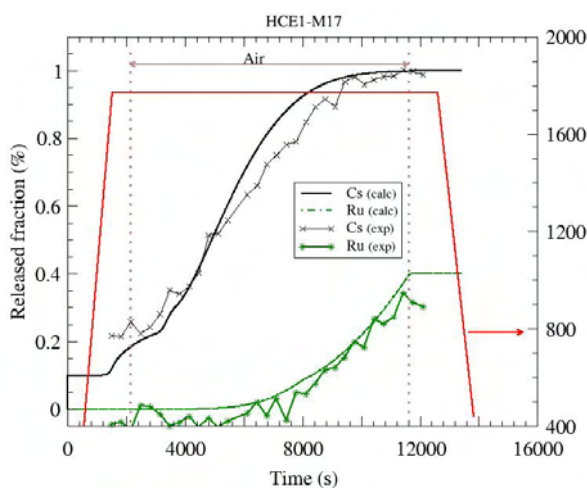


Figure 6: Release kinetics of Cs and Ru for test HCE1-M17.

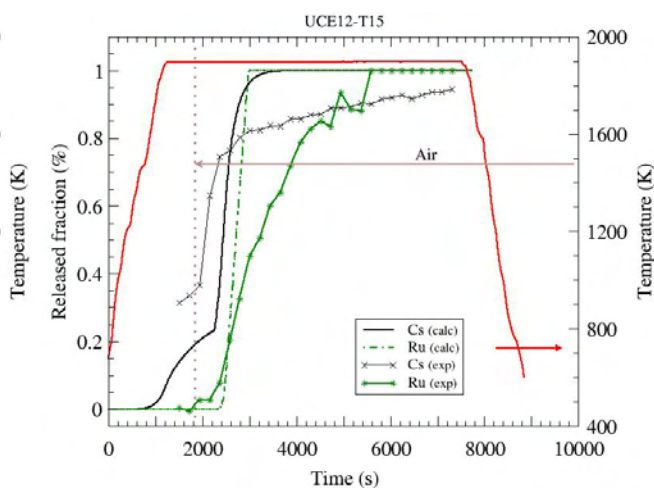


Figure 7: Release kinetics of Cs and Ru for test UCE12-T15.

B.3 Ruthenium transport in the RCS

Once released from the fuel, ruthenium will pass through lower temperature areas in the primary circuit. Previous experiments conducted at VTT and at AEKI, devoted to the study of the formation and transport of volatile ruthenium oxides by exposing RuO_2 powders to diverse air-mixed atmosphere, proved that the amount of gaseous ruthenium reaching the containment through its transport in such strong temperature gradient was significant at certain conditions. Therefore, the transport of ruthenium tetroxide has been specifically studied at VTT by injecting directly gaseous RuO_4 into the facility (Ref. [24]) to study its decomposition, while the effect of other FPs on transport of ruthenium has been investigated at AEKI (Ref. [26]).

B.3.1 Gaseous RuO_4 injection experiments

In these VTT experiments, the specific interest was the influence of surface material on RuO_4 transport and retention. The tube material in the experimental reactor (hot zone) was high-purity alumina. The set-point of the furnace was 1500 K. Downstream of the reactor, the

Source Term and Containment Issues, Paper 3.9

gas temperature decreased to about 360 K. The tube material (64 cm) used after the furnace was either alumina or stainless steel (SS 316 L). In addition, the effect of oxidation and RuO₂ aerosol deposition on steel surface was studied by placing sample plates in the tube. Moreover, in the same experiment, CsI powder was placed in an alumina crucible. Ruthenium retention was measured by using radioactive tracer in three experiments out of four.

Gaseous RuO₄ was produced in a distillation flask. The procedure was to first dissolve RuCl₃ in concentrated HCl-water solution. The solution was mixed with concentrated H₂SO₄. By heating the flask gently, chlorine was distilled out of the solution. RuO₄ gas could then be produced by adding a drop of oxidizing agent KMnO₄ or H₂O₂. Air flow of 1 l/min (NTP) carried the produced RuO₄ gas into the facility. Before entering the furnace, carrier gas was mixed with air flow of 4 l/min (NTP) that had been saturated at 30°C with water in a thermostated bubbling bottle. The amount of produced gaseous ruthenium injected into the inlet of the facility ranged from 2 to 23 mg. The rate of gaseous RuO₄ injection depended on the oxidation procedure

At the end of the high temperature furnace, the gas flow began to cool down, as one could expect from the exit of a reactor core vessel down to the primary circuit break. Gaseous RuO₄ decomposed partly and formed RuO₂ particles. Nucleated aerosol particles were collected on plane filter at location 106 cm downstream of the furnace. Gaseous ruthenium was trapped downstream of the filter in a 1 M NaOH-water solution.

In experiments with an alumina tube, the fraction of gaseous ruthenium transported beyond the tube line ranged from 45% to 51% of ruthenium injected. The rest of the produced gaseous ruthenium mostly reacted with surfaces, as aerosol formation was generally rather small. When the alumina tube was replaced with a stainless steel (SS) tube, the fraction of gaseous ruthenium transported through the tube line decreased to 13% of ruthenium injected. Stainless steel thus catalysed the reaction of RuO₄ on its surface to RuO₂ as well as formation of aerosol particles. The fraction of transported RuO₂ aerosols to filter doubled to 6.7% compared to experiments with alumina tube. In the injection experiments, ruthenium oxides did not reach thermo-dynamic equilibrium within the facility at 1500 K, and likely also downstream, as in some cases a quite significant fraction of gaseous ruthenium was trapped in the bubbler.

In the last experiment, altogether eight SS-plates (15 mm x 20 mm) were placed within the alumina tube at two locations, 30 cm and 55 cm downstream of the furnace. Four of the eight plates were oxidised at 1000°C in steam flow and four had metallic surface. Before the experiment, RuO₂ particles were deposited on top of two oxidised plates and two metallic plates. Four differently prepared plates were used at both locations. The surface of the sample plates with aerosol deposits was analysed with X-ray photoelectron spectroscopy (XPS) to confirm that the ruthenium layer on plates was in the form of RuO₂. The amount of ruthenium deposited on different sample plates during the experiment could be determined from the activity of the plates, since part of the ruthenium injected into the facility was activated before the experiment.

As an example of the results, the fraction of injected ruthenium deposited on SS-plates is presented in figure 8. In brackets is presented the proportion of ruthenium deposited on a single plate of the total amount of deposited ruthenium at both locations.

Source Term and Containment Issues, Paper 3.9

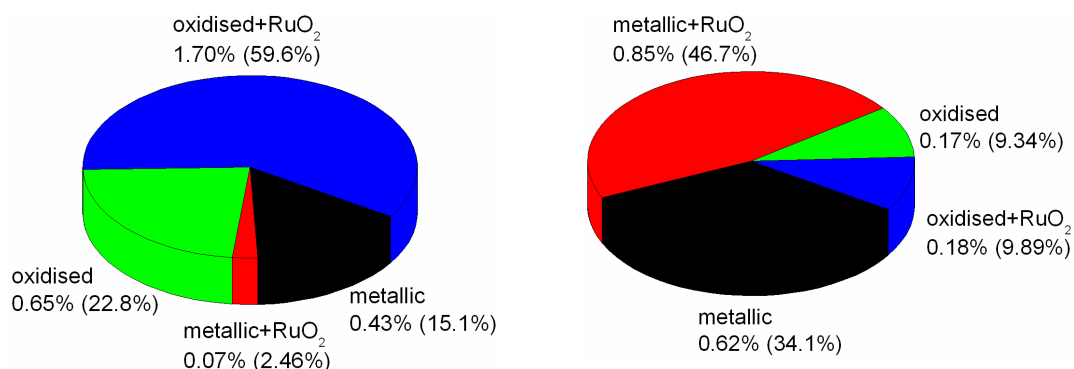


Figure 8: The fraction of injected gaseous ruthenium deposited on SS-plates. Sample plates were placed downstream of the furnace at 30 cm on the left and 55 cm on the right. The proportion of ruthenium deposited on single plate of the total amount of deposited ruthenium at each location is presented in brackets.

According to the results, at the higher temperature (location 30 cm), the oxidised surface was more efficient in trapping ruthenium than the metallic surface. Pre-deposited RuO₂ particles further increased ruthenium retention on oxide surface. On the metallic surface, RuO₂ particles significantly inhibited the retention of ruthenium. An oxidised SS-plate prepared with RuO₂ deposits trapped 24 times more ruthenium than similarly prepared metallic plate placed on the opposite wall of the tube. Such a great difference is not explained by aerosol deposition processes and therefore has to be a result of difference in RuO₄ reaction on the surface. At lower temperature (location 55 cm) the situation was reversed. The amount of trapped ruthenium on metallic surface was greater than on oxidised surface. Pre-deposited RuO₂ particles seemed to slightly increase retention of ruthenium on metallic surface. The observed dependence of RuO₄ reaction on the temperature of SS surface agrees very well with the previously measured ruthenium deposition data. A deposition peak was usually formed at 30 cm to 37 cm from the outlet of the furnace as the temperature of the metallic stainless steel tube decreased enough to allow reaction of RuO₄ on its surface, see Fig. 9. During the experiment, a crucible filled with CsI powder (mass 1 g) placed inside the alumina tube at location 65-90 cm after the furnace trapped 0.74 mg (3.3 % of injected gaseous Ru) of ruthenium, most likely in the form of Cs₂RuO₄.

B.3.2 Analysis of VTT ruthenium transport experiments

To start with the analysis of these ruthenium experiments, the temperature profile inside the facility was measured (Ref. [25]). Several specific measurements were conducted and as a result accurate thermal boundary conditions could be defined for computational fluid dynamics (CFD) modelling. As modelling of all the phenomena mechanistically was impossible at this stage, transport and deposition of RuO₂ and RuO₃ were assumed to be purely diffusion limited. The kinetics of ruthenium conversion to RuO₄ were assumed to be so slow that the conversion is of secondary importance during the relatively brief cooling phase. The role of RuO₄ is considered only in the analysis of the results. As a further simplification, only

Source Term and Containment Issues, Paper 3.9

condensation on the reactor surfaces was considered by adopting a wall boundary condition of equilibrium concentration above the surface. The modelled cases were chosen from previous experiments with dry air (Ref. [24]). Since RuO_3 is the dominant species, the effective vapour pressure was calculated by converting the equilibrium concentration of RuO_2 to RuO_3 , and adding this to the equilibrium RuO_3 concentration. Since RuO_3 does not have a condensed form, the estimate of RuO_4 diffusion coefficient was also adopted for RuO_3 .

The simulated deposition profiles and experimental data are presented in figure 9. As the computational grid was rather coarse, no conclusions should be made based on the exact shapes of the peaks or the occurrence of minor peaks. The comparison shows however that there is a reasonable agreement with the modelling results and the experimental data especially at 1500 K. According to the modelling of the thermal fields and gaseous ruthenium concentrations (as RuO_3), the sharp beginning of wall deposition is clearly visible. It seems that the hypothesis of the dominant roles of RuO_2 and RuO_3 is valid and the first deposition peak can be estimated as diffusion limited condensation. The fact that experimentally observed level of deposition is much lower at 1300 K than at 1500 K is most likely at least partly due to greater gas phase RuO_4 concentration at that temperature. In equilibrium, the RuO_4 mass fraction of gas phase ruthenium species is 25 % at 1300 K, while only 9 % at 1500 K. Even if the experiments show that equilibrium is not reached in the RuO_4 to RuO_3 reaction, it does not necessarily mean that the reaction from RuO_3 to RuO_4 could not approach the equilibrium within the time scale of the heated furnace.

Particle formation can be observed in the comparison of the simulations and the experimental data. Particles start to have an impact at the furnace outlet (0 cm). Based on pure vapour diffusion, deposition rates should level off at this location. It seems logical that, in reality, most of the RuO_2 and RuO_3 vapour is scavenged by particles here, and that is why the deposition rates decrease further. According to modeling, buoyancy plays a role at the outlet of the furnace. The hot gas flow is directed towards the top of the furnace. During the experiments an important fraction of nucleation has most likely taken place rather close to the upper wall of the tube. Due to the high temperature gradient these particles have had a rather high propensity of ending up as wall deposits. In the experimental data there is a visible peak of particle deposition due to thermophoresis.

However, this scenario is far from a complete explanation for the observed RuO_4 transport rates. The third deposition peak in experimental data is probably formed due to decomposition of RuO_4 to RuO_2 on stainless steel surface at about 100-150°C. Decomposition seems to be enhanced on metallic surface by deposited RuO_2 particles. RuO_4 was not considered in this modelling.

Source Term and Containment Issues, Paper 3.9

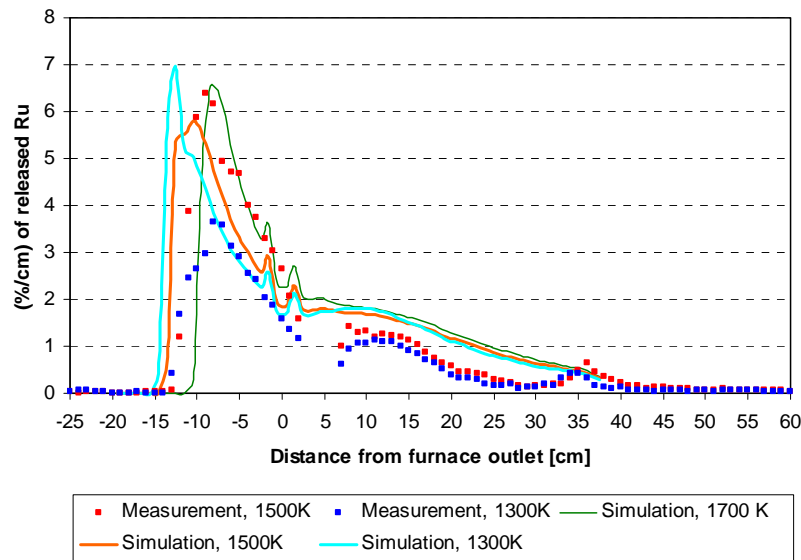


Figure 9. Deposition profiles simulated using Fluent CFD compared with measured ruthenium deposition.

B.3.3 Experimental study of other FPs influence on ruthenium transport experiments

The previous RUSSET (RUthEnium SEparate EEffect TEst) experiments performed at AEKI (Ref. [26]) proved that other fission products and UO_2 can influence both the amount of RuO_4 reaching the reactor containment (evidenced by the concentration of RuO_4 measured at ambient temperature at the exit of the AEKI facility) and can cause a time delay in appearance of maximum values of this concentration. The main objectives of the last test series (RUSSET-6) were identification of those fission products which play a role in this time delay. Effects of four characteristic groups of fission product elements (see Table I) on the behaviour of Ru in high temperature air atmospheres were investigated. Above the high temperature, solid-state reactions in the reaction chamber, presumably reactions in the decreasing temperature outlet area, delayed the release of Ru in the escaping cooled down air.

Ru + Cs compounds (CsI , Cs_2CO_3)
Ru + Ba compounds (BaO / BaCO_3)
Ru + metals (Mo, Se, Sn, Ag, Sb, Cd, Te)
Ru + rare earth oxides (Nd_2O_3 , CeO_2)

Table I. Four characteristic groups of fission product elements

Source Term and Containment Issues, Paper 3.9

The samples consisted of solid-state mixtures of the investigated fission product elements and metallic ruthenium powder in a ZrO_2 matrix. The applied concentrations of inactive fission product components represented medium burn-up fuel (44 MWd/kgU). In each test, 1 g ZrO_2 with mixtures of fission product elements containing ~ 5 mg Ru was filled as a charge into the reaction chamber. Air injection ($171 \text{ cm}^3/\text{min}$) started when the furnace with sample was heated up to the required temperature. Isothermal experiments were performed at 1000 and 1100°C.

The released ruthenium was collected in two places: in an inner quartz tube placed into the outlet tube of reaction chamber to determine the amount of deposited RuO_2 in the decreasing temperature area, and in an ambient temperature absorber solution at the outlet to quantify the gaseous ruthenium oxide components in the outlet gas after cooling down. Both the inner quartz tube and the absorber solution were changed at the same time to assess the RuO_x escape from the furnace area as a function of time. To understand the chemical reactions in the decreasing temperature outlet area and the thermo-chromatographic effects, a quartz rod of 2 mm diameter was placed into the first applied quartz inner tube. The outer surface of the quartz rods was investigated by the micro-beam X-ray fluorescence (μ -XRF) technique in order to determine the axial distribution of the inactive simulated fission elements deposited along the sampler rods.

In presence of molybdenum in the charge, the fraction of ruthenium measured in the absorber solution was about 13% in the 1100°C (test No. 15 and 17), and about 40% in the 1000°C (test No. 18), while using MoO_3 covered sampling tubes, this part was only ~ 7% in the 1100°C (test No. 24). In the vapour phase, simultaneously present molybdenum oxides decrease the surface-catalysed decomposition of RuO_x and result in nearly one order of magnitude higher RuO_x partial pressures in the ambient temperature escaping air as in case of pure Ru oxidation (see Figure 10.). The scanning results showed that MoO_3 and TeO_2 deposited together in temperature range 600 to 300°C. At this area, large RuO_2 crystals grew, which is usually typical at the higher temperature region.

Caesium seems to be the fission product element which plays the main role in causing the time delay in appearance of ruthenium oxides in the ambient temperature escaping gas (see Figure 11). In the presence of caesium compounds, the maximum concentration of RuO_4 in the outlet air appeared between 30-60 min at 1100°C (at sampling frequency 30 min). The interpretation of results obtained at 1000°C (there was no time delay) and at a sampling frequency of 15 min at 1100°C (see Figure 11) needs more investigations. Test No. 12 was performed in the same device as the previous test No. 11, which probably influenced the results because of high temperature interactions between Cs and the quartz wall of the reaction chamber. The Cs deposition occurred on every investigated quartz rods in temperature range ~ 800 to 300°C.

In presence of barium and rare earth oxides barium, ruthenate and rare earth ruthenates form which cause lengthened Ru escape from the high temperature area and probably also result in time delay in the appearance of the maximum concentration of RuO_4 in the outlet air.

Although these results are still being interpreted, it appears clear that reactivity of ruthenium oxides with other chemical compounds such as caesium or molybdenum will affect their transport in the RCS to the containment.

Source Term and Containment Issues, Paper 3.9

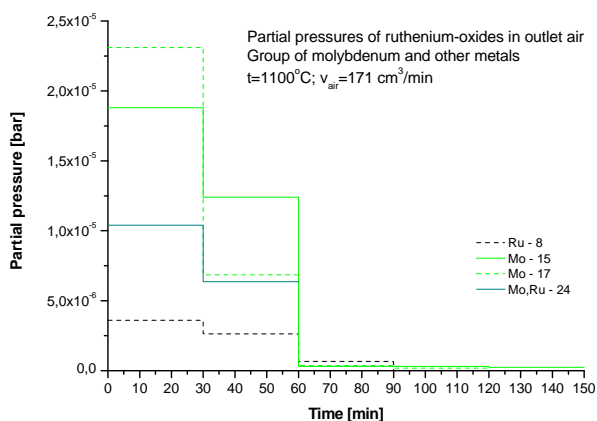


Figure 10. Partial pressures of RuO_4 in outlet air group of molybdenum and other metals

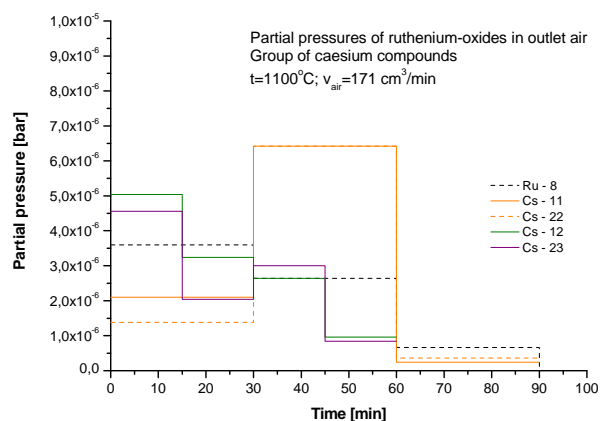


Figure 11. Partial pressures of RuO_4 in outlet air group of caesium compounds

Finally, it must be emphasised that both series of experiments (VTT and AEKI) clearly demonstrated that the decomposition process of RuO_4 to RuO_2 was not completed and did not follow equilibrium. There were therefore kinetic limitations, and as a first investigation step, a comparison of transit times of transported ruthenium oxides molecules from the hotter zones (furnace areas) to colder zones (liquid traps) was carried out. For both series of experiments, the temperature profile as a function of the distance from the end of the furnace was determined. In the case of the VTT experiments, for a 5 l/min flow, the temperature variation as a function of the time was calculated, considering the diameter of the furnace is 22 mm. This is represented in figure 12 from which one can see that the time for a single particle or group of particles to arrive from the release point to the cold zone is about 3 seconds. For the RUSSET experiments, the temperature kinetic was calculated for the most representative tests. In this case, the tube diameter was 14 mm. Values of the air flow were 0.06, 0.17, 0.3, 0.4, 0.6 and 0.9 l/min and the temperatures went from 1373 to 1973 K. Some of the results are shown in figure 13. The time for particles to reach the cold zone was found to be from one to four seconds (only the experiment with the lowest flow rate of 0.06 l/min gives a time of ten seconds). These transit times are within the range of those from the core outlet zone to the reactor containment zone calculated for typical loss of coolant accidents (LOCA) with a break located at the hot leg of the reactor coolant system (RCS) or at the Pressurized Operated Valves of a Pressurizer. It is thus quite likely that volatile ruthenium oxides will reach the containment after an air ingress into the core vessel.

Source Term and Containment Issues, Paper 3.9

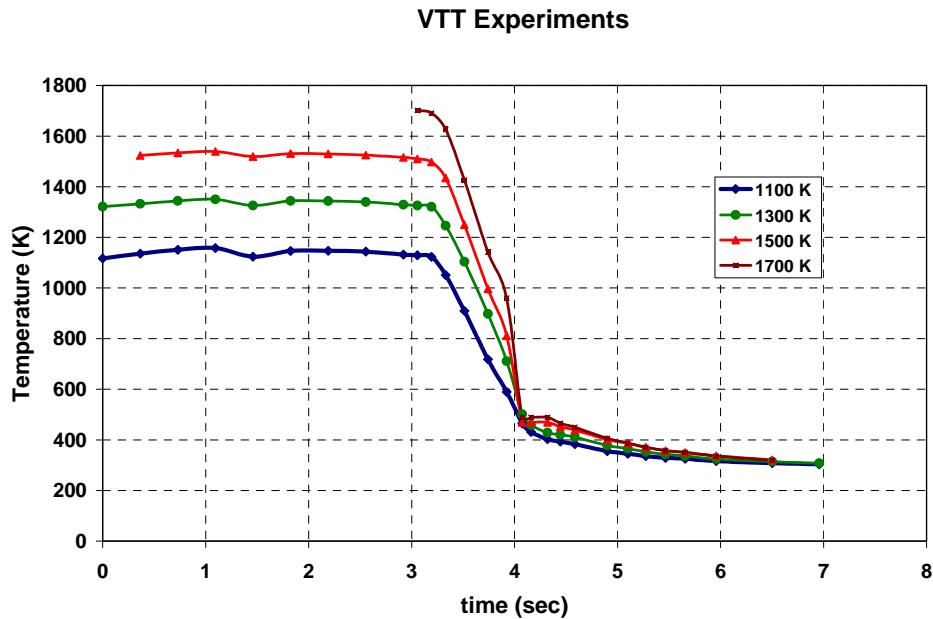


Figure 12: Transit time for molecules through the temperature gradient in the VTT tests

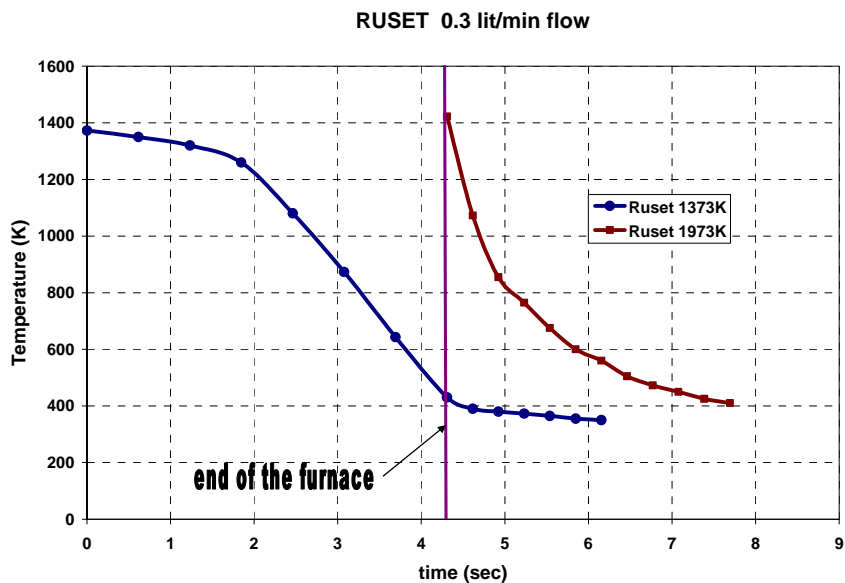


Figure 13: Transit time for molecules through the temperature gradient in the RUSET tests

B4 Ruthenium behaviour in the reactor containment

From elements reported in B.3, it comes clear that ruthenium will reach the reactor containment building under different forms. As previously stated, the literature review revealed a lack of quantified data on RuO_4 gaseous phase stability at low temperatures such as ones encountered in reactor containments, and on behaviour of the oxides $\text{RuO}_2(\text{c})$ and $\text{RuO}_4(\text{g})$ in radiolytic conditions. Therefore, an experimental programme aiming at better understanding of the physicochemical behaviour of ruthenium species was launched.

Source Term and Containment Issues, Paper 3.9

B.4.1. Study of RuO₄(g) stability

Although gaseous ruthenium tetroxide is often described as an "unstable" species, its stability has to be evaluated on a severe accident timescale, i.e. during the first 24 hours after the reactor scram and thereafter. For this purpose, a reliable and reproducible method of generating pure ruthenium tetroxide crystals was firstly developed, since this compound is not available commercially. Experimental results show that RuO₄(g) decomposition is slower than would be expected, based on the few indications given in the literature. Thus, in conditions representative of containment during a severe accident, i.e. at least 90°C and in the presence of steam, half-life time for the gaseous tetroxide is around five hours. Furthermore, decomposition does in fact appear to follow a first-order rate law relative to the RuO₄ concentration, as predicted by certain authors (Refs. [27], [28]), even if their results were obtained in different conditions. Regarding substrate interactions, the results contradict other findings in the literature, showing that RuO₄(g) has no special affinity with ferrous substrates or epoxy paints. In fact, the type of substrate has no influence on gaseous tetroxide decomposition kinetics (Ref. [29]). This is quite different from what is observed at higher temperature in the RCS (cf. B3). Finally, the tetroxide decomposition reaction is accelerated by the presence of steam and deposits of ruthenium oxides (RuO₂ or similar compounds), which act as catalysts.

B.4.2. Ruthenium deposit surface characterization

X-ray photoelectron spectroscopy (XPS) was used to analyze the deposits resulting from the interactions between RuO₄ and the two PWR containment substrates. The findings led to the following conclusions:

- there is strictly no difference in the types of ruthenium species found in deposits on epoxy paint and stainless steel,
- there are no chemical bonds linking the deposited ruthenium to the paint polymer or the iron oxides; in other words, no chemical reaction takes place at the deposit surface.

XPS spectra also established that the species deposited on the two containment substrates were similar to those detected in the commercially available reference sample of hydrated ruthenium dioxide. Analysis of the Ru3d and O1s orbitals indicated that hydroxylated forms of Ru(IV), e.g. RuO(OH)₂, made up most of the Ru deposits (at least at the outermost surface, i.e. \approx 10 nm). They are the only species whose presence can be explained in both the commercial hydrated Ru dioxide reference powder and the experimental samples (Ref. [30]). These results, coupled with the RuO₄(g) stability results, led to conclude that ruthenium tetroxide decomposition is a direct gas phase process, followed by condensation of the reaction products on surfaces, rather than a classical adsorption process. Using XPS analysis and taken into account scarce indications in the literature, a preliminary mechanism of RuO₄(g) decomposition was proposed (Ref. [29]).

B.4.3. Ruthenium deposit oxidation study

The stability of containment ruthenium deposits in accident conditions, i.e. in a partially oxidizing environment, was investigated using two approaches. The first one consists in performing tests without irradiation, using an ozone generator to determine Ru deposit oxidation kinetics constants, under the effect of ozone. The second one consists in conducting radiolytic tests in the irradiation facility EPICUR (Ref. [31]). This irradiator delivers a dose of around 4 kGy/h, aiming at realistically reproducing physicochemical containment conditions during an accident, particularly the inventory of radiolysis products (OH[•], O₃, etc.).

Source Term and Containment Issues, Paper 3.9

The first qualitative study, involving the ozone generator, highlighted the phenomenon of revolatilization from ruthenium oxide deposits in the 40°C-90°C temperature range, in both dry and moist air. Revolatilization was induced by the oxidizing effect of O₃ on active Ru deposit sites, producing RuO₄(g). The same oxidation reaction was also detected in radiolysis tests, under the same temperature and humidity conditions. Thus, it was experimentally shown that temperature and humidity represent two key factors, whether or not ionizing radiation is present. More specifically, increasing these two parameters clearly favours the oxidation reaction. The strong effect of an increased humidity rate is assumed to be attributable to the hydroxyl radical (OH[•]), which is an extremely powerful oxidizing agent. Based on the ozonation tests, an oxidation rate law of ruthenium deposits was proposed. This oxidation reaction is a partial first-order reaction with respect to [O₃] and [H₂O] (Ref. [32]).

Based on the rate laws established during the study without irradiation (RuO₄(g) decomposition and oxidation of the deposits forming again RuO₄(g)), but nonetheless in the presence of radiolysis products (from O₃), the predictive Ru fractions revolatilized under irradiation were calculated, then compared with the experimental irradiation results obtained in EPICUR. The calculated fractions were under-estimated by about one order of magnitude. Therefore, oxidation is enhanced under γ-radiolysis as compared to the ozonation tests; this is explained by the predominant role of the O[•] and/or OH[•] radicals. Indeed, during the γ-radiation tests, additional quantities of these radicals are produced directly by air and steam radiolysis. An updated radiolytic oxidation rate law for ruthenium deposits was thus proposed (Ref. [33]).

B.4.4. Ru behaviour in the sump

After having reached the containment building atmosphere, part of the ruthenium species will settle in the sump. Oxidation of ruthenium species in this aqueous phase is also conceivable, to the extent that radiolysis, as induced by suspended or dissolved fission products, can transform the “water” into an oxidizing medium. The sump would then constitute a potential source of volatile ruthenium (typically RuO₄(g)).

Some experimental irradiation tests have thus been performed in the EPICUR facility, in order to evaluate such phenomena. Three species of ruthenium have been studied: dissolved powder of KRuO₄ representative of ruthenium aerosols, RuO₂(s) and RuO₄(aq). The temperature of 90°C was used for all tests and realistic concentrations of Ru were selected (10⁻³/10⁻⁴ mol.L⁻¹). The effect of the sump pH was also investigated (values 5 and 9).

The main outcomes resulting from these irradiation tests indicated that no Ru volatilization occurred from both aqueous solution of RuO₂.2.6H₂O and RuO₄⁻, whatever the sump pH. Concerning the behaviour of RuO₄(aq) aqueous samples (made by dissolution of RuO₄ vapours), the situation is different as, in basic conditions (pH of 9), 75% of Ru was volatilized for a 16 hours irradiation. Moreover, note that about 50% of Ru was volatilized for a 31 hours heating at 90°C without any irradiation. A strong impact of heating was thus highlighted and it can be said that γ-radiations act only as a booster agent for the revolatilisation phenomenon. This effect of temperature was also confirmed by an UV-visible spectroscopy study, showing that about 50% of Ru was volatilized from RuO₄(aq) at 10⁻⁴ M, for a 24 hours heating at 90°C. In addition, this last study showed that no formation of new aqueous species from RuO₄(aq) occurred during heating, evidencing that Ru volatilization occurred directly from RuO₄(aq). A question remains in the case of an acidic sump (pH of 5), this point will be investigated in a soon future. At the present time, it can be concluded that the sump is an efficient trap for ruthenium aerosols species, while it is not for RuO₄(g) (at least for basic conditions of pH).

Source Term and Containment Issues, Paper 3.9**C. CONCLUSIONS**

Air ingress is potentially relevant to all core melt accidents for which in-vessel flooding cannot be performed or is not successful in recovering the core to a safe and controlled state. Probabilities of such situations are small, but high enough to warrant consideration. The topic has therefore been addressed right through the SARNET project, in a dedicated Work Package of the Source Term Topical area and the work carried out has been regularly reported (Refs. [2], [3]); this paper is the final contribution.

Such air ingress situations have significant implication for the source term as there is a non-negligible risk of having some solid fuel remaining in the vessel after a lower head failure, with significant amount of metallic inclusion of ruthenium inside (in TMI-2, more than half the reactor core stayed in place in the upper and peripheral region of the active core area). This ruthenium, when exposed to a very oxidising environment like air, can form volatile oxide species, and it was shown that these species were able to reach containment building, where gaseous forms can persist due to different radio-chemical reactions.

Thanks to many experimental investigations performed by partners, with experimental conditions and matrices debated within the group, predictive models for material cladding oxidation, UO_2 oxidation and subsequent ruthenium release, have been proposed for future integration in ASTEC. The basis for a future predictive model for the ruthenium transport in the reactor coolant system is emerging from the interpretation of dedicated VTT and AEKI tests. A set of equations to model and capture the main behaviour of ruthenium species in the containment building has been developed, from ISTP results.

In that view, significant achievements have been reached.

However, this issue cannot be considered as completely solved. Some remaining key questions have been identified, and partners came to a consensus on a work programme in the proposed follow-up programme SARNET2, to solve finally the issue.

One concern is the FP release from high burn-up and MOX fuels and under mixed steam-air conditions, which are more realistic than 100% air conditions studied up to now in accident situations. Although mixed-air atmosphere oxidation of Zircaloy has already been studied, the oxidation of the fuel itself is a field not investigated up to now, which needs attention as the evolution of fuel management tends towards these type of fuels. Concerning ruthenium transport in RCS, thermodynamic behaviour of ruthenium oxides in regards with reactivity with surfaces and other chemical compounds such as caesium or molybdenum still needs some more investigations, from RUSSET test findings. Kinetics of decomposition of RuO_4 have also to be studied as it is likely that short transit times from hot zones to cold zones would occur in reactor situations. Among the unresolved questions remains also the potential release of previously deposited FPs (during the so-called in-vessel phase of the accident) which would partly be volatilised when exposed to oxygen, possibly inducing a delayed release to the containment. This is likely to occur not only for ruthenium deposits but also for elements such as iodine. Revaporisation investigations are thus proposed in SARNET2.

Acknowledgements

This work has been conducted under contract SARNET FI6O-CT-2004-509065.

References

[1] F. C. Iglesias, C. E. L. Hunt, F. Garisto, D. S. Cox, N. A. Keller, R. D. Barrand, J. R. Mitchell and R.F. O'Connor, "Measured Release Kinetics of Ruthenium from Uranium

Source Term and Containment Issues, Paper 3.9

- Oxides in Air and Steam”, Seminar on Fission Product Transport Processes During Reactor Accidents, Editor Hemisphere Publishing Corp. Washington, 1990.
- [2] A. Auvinen, N. Davidovich, G. Ducros, Y. Dutheillet, M. P. Kissane, L. Matus and A. Rizoïu “On-going Investigation of Ruthenium Release and Transport”, 1st European Review Meeting on Severe Accident Research (ERMSAR-2005), Aix-en-Provence, France, Nov. 2005.
- [3] A. Auvinen, G. Brilliant, N. Davidovich, G. Ducros, R. Dickson, Y. Dutheillet, P. Giordano, T. Kärkelä, M. Mladin, Y. Pontillon and C. Séropian, “Progress on Ruthenium Release and Transport under Air Ingress Conditions”, 2nd European Review Meeting on Severe Accident Research (ERMSAR-2007), Forschungszentrum Karlsruhe GmbH (FZK), Germany, 12-14 June 2007.
- [4] P. Taylor, “Thermodynamic and Kinetic Aspects of UO₂ Fuel Oxidation in Air at 400-2000 K”, J. Nucl. Mater. **344**, pp. 206-212, 2005.
- [5] C. Mun, L. Cantrel and C. Madić, “Review of Literature on Ruthenium Behaviour in Nuclear Power Plant Severe Accidents”, Nuclear Technology **156 (3)**, pp. 332-346, 2006.
- [6] M. Steinbrück et al., “Experiments on Air Ingress during Severe Accidents in LWRs”, Nucl. Eng. Design **236**, pp. 1709-1719, 2006.
- [7] G. Schanz et al., “Results of the QUENCH-10 Experiment on Air Ingress”, Forschungszentrum Karlsruhe, Report FZKA 7087, 2006.
- [8] O. Coindreau, C. Bals, E. Beuzet, J. Birchley, S. Ederli, T. Haste, T. Hollands, M. K. Koch, J-S. Lamy and K. Trambauer, “Modelling of Accelerated Cladding Degradation in Air for Severe Accident Codes”, 3rd European Review Meeting on Severe Accident Research (ERMSAR-2008), Nesseber, Bulgaria, 23-25 September 2008.
- [9] D. Ohai, “Fission Product Release from Debris Bed (FIPRED) Project Description”, SARNET-ST-P53, INR Report No 7734/2006, 2007.
- [10] D. Ohai, I. Dumitrescu and T. Meleg, “FIPRED: Preliminary Tests on UO₂ Sintered Pellets Disintegration”, SARNET-ST-P56, 2007, INR Report No 7735/2007.
- [11] D. Ohai, I. Furtuna and T. Meleg, “Advances in FIPRED Results at High Temperature”, SARNET-ST-P68, INR Report 8048/2007, 2008.
- [12] Y. Pontillon, “Semi-Volatile FP Release from VERCORS Tests”, International VERCORS Seminar, Gréoux-les-Bains, France, September 2007.
- [13] G. Brilliant, “Interpretation and Modelling of Fission Products Behaviour in VERCORS Tests”, International VERCORS Seminar, Gréoux-les-Bains, France, September 2007.
- [14] M. S. Veshchunov, V. D. Ozrin, V. E. Shestak, V. I. Tarasov, R. Dubourg and G. Nicaise, “Development of the Mechanistic Code MFPR for Modelling Fission-Product Release from Irradiated UO₂ Fuel”, Nucl. Eng. Design, **236(2)**, pp. 179-200, 2006.
- [15] G. Brilliant, “Modélisation de l'Oxydation et de la Réduction du Combustible sous Vapeur d'Eau et sous Air”, IRSN Tech. Report SEMIC-2007-383, 2007.
- [16] J. C. Ramirez, M. Stan and P. Cristea, “Simulations of Heat and Oxygen Diffusion in UO₂ Nuclear Fuel Rods”, J. Nucl. Mater. **356**, pp. 174-184, 2006.
- [17] P. Ruello, K. D. Becker, K. Ullrich, L. Desgranges, C. Petot and G. Petot-Evars, “Thermal Variation of the Optical Absorption of the Small Polaron Self-Energy”, J. Nucl. Mater. **328**, pp. 46-54, 2004.
- [18] D. Labroche, O. Dugne and C. Chatillon, “Thermodynamics of the U-O System. I – Oxygen Chemical Potential Critical Assessment in the UO₂-U₃O₈ Composition Range”. J. Nucl. Mater. **312**, pp. 21-49, 2003.
- [19] D. S. Cox, C. E. L. Hunt, Z. Liu, N. A. Keller, R. D. Barrand, R. F. O'Connor and F.C. Iglesias, “Fission Product Releases from UO₂ in Air and Inert Conditions at 1700-2350 K:

Source Term and Containment Issues, Paper 3.9

- Analysis of the MCE-1 Experiment”, in Safety of Thermal Reactors, Amer. Nucl. Soc. Int. Topical Meeting (also published as report AECL-10438), 1991.
- [20] R. D. Barrand, R. S. Dickson, Z. Liu and D.D. Semeniuk, “Release of Fission Products from CANDU Fuel in Air, Steam and Argon Atmospheres at 1500-1900°C: The HCE3 Experiment”, Proc. 6th Intl. Conf. on CANDU Fuel, pp. 271-280, 1999.
- [21] R. S. Dickson, Z. Liu, D. S. Cox, N. A. Keller, R. F. O'Connor and R. D. Barrand, “Cesium Release from CANDU Fuel in Argon, Steam and Air: The UCE12 Experiment”, Proc. 15th Annual Canad. Nucl. Soc. Conf. (also published as AECL-CONF-00085), 1994.
- [22] D. S. Cox, Z. Liu, P. H. Elder, C. E. L. Hunt and V. I. Arimescu, “Fission-Product Release Kinetics from CANDU and LWR Fuel During High-Temperature Steam Oxidation Experiments”, Fission Gas Release and Fuel Rod Chemistry Related to Extended Burnup, IAEA-TECDOC-697, 1993.
- [23] C. E. L. Hunt, D. S. Cox, Z. Liu, N. A. Keller, R. D. Barrand, R. F. O'Connor and F. C. Iglesias, “Ruthenium Release in Air”, Proc. 12th Canad. Nucl. Soc. Conf., 1991.
- [24] T. Kärkelä, U. Backman, A. Auvinen, R. Zilliacus, M. Lipponen, T. Kekki, U. Tapper and J. Jokiniemi, “Experiments on the Behaviour of Ruthenium in Air Ingress Accidents – Final Report”, VTT report VTT-R-01252-07, 2007.
- [25] T. Kärkelä, J. Pyykönen and A. Auvinen, “Analysis of Flow Fields, Temperatures and Ruthenium Transport in the Test Facility”, VTT report VTT-R-00947-08, 2008.
- [26] N. Ver, L. Matus, M. Kunstár, J. Osan and Z. Hózer, “Delay of Ruthenium Escape in the Presence of some Fission Product Elements”, AEKI report AEKI-FRL-2007-409-01/01, SARNET-ST-P63, November 2007.
- [27] A. Ortins de Bettencourt and A. Jouan, “Volatilité du Ruthénium au Cours des Opérations de Vitrification des Produits de Fission (2ème partie)”, Rapport CEA-R-3663 (2), CEN de Fontenay-aux-Roses, 1969.
- [28] H. Debray and A. Joly, “Compte Rendu des Séances de l'Académie des Sciences **1888(106)**, pp. 328-333.
- [29] C. Mun, L. Cantrel and C. Madic, “Study of RuO₄ Decomposition in Dry and Moist Air”, Radiochimica Acta. **95(11)**, pp. 643-656, 2007.
- [30] C. Mun, J. J. Ehrhardt, J. Lambert and C. Madic, “XPS Investigations of Ruthenium Deposited onto Representative Inner Surfaces of Nuclear Reactor Containment Buildings”, Applied Surface Science **253(18)**, pp. 7613-7621, 2007.
- [31] S. Guilbert, L. Bosland, D. Jacquemain, B. Clément, F. Andreo, G. Ducros, S. Dickinson, L. Herranz and J. Ball, “Radiolytic Oxidation of Iodine in the Containment at High Temperature and Dose Rate”, Nuclear Energy for New Europe 2007, Portoroz (Slovenia), September 2007.
- [32] C. Mun, L. Cantrel and C. Madic, “Oxidation of Ruthenium Oxide Deposits by Ozone”, Radiochimica Acta. **96**, pp. 375-384, 2008.
- [33] C. Mun, L. Cantrel and C. Madic, “Radiolytic Oxidation of Ruthenium Oxide Deposits”, Accepted for publication in Nuclear Technology, 2008.